Evacuated Spheres for Closed-Cell Vacuum Insulation

Diana Hun, PhD, PE (inactive) **Tomonori Saito, PhD** **James Klett, PhD**

Tolga Aytug, PhD **Kai Li, PhD** **Bingrui Li**

Som Shrestha, PhD, BEMP **Kaushik Biswas, PhD** **Soydan Ozcan, PhD**
Member ASHRAE

ABSTRACT

Insulation materials with a thermal resistance per inch higher than 6 h·ft²· °F/Btu·in. or R6/in. (42 m·K/W) are needed for building envelope retrofits in which solutions with slim profiles are required because of minimal available space or because real estate has a premium cost. These insulation materials will also be of benefit to prefabricated construction given that slim designs either reduce shipping costs or increase the floor space provided to the customer. Vacuum insulation panels (VIPs) are the current state-of-the-art insulation material with a resistance of about R35/in (243 m·K/W); however, their use in buildings is hindered by the fact that damages to their protective film decrease their performance to ≤R8/in (56 m·K/W). Given the lack of robust, highly-insulating materials, we are exploring methods to develop evacuated spheres that can act as a closed-cell vacuum insulation. The evacuated spheres could be assembled into boards that could attain ~R14/in (97 m·K/W). Advantages that evacuated spheres will offer over VIPs are that they will likely be more suitable for construction because punctures will only cause localized damage, and that the boards could be cut into customized shapes. We are currently investigating two processes to evacuate spheres to produce polymeric vacuum insulation spheres (PVISs) and coated and evacuated insulation spheres (CEISs). PVISs involve the extrusion of economical polymers, blowing agents, and gas barriers. CEISs use naturally-occurring or synthesized hollow particles with porous shells that are evacuated and coated with a gas impermeable thin film. Both manufacturing processes aim for very large throughputs to ensure cost-effectiveness and adoption by the construction industry. This paper discusses the manufacturing techniques that we are exploring and our progress to date.

INTRODUCTION

The construction industry, and in particular envelope retrofits and prefabricated (i.e., panelized and modular) systems, will benefit from insulation materials that have higher than R6/in (42 m·K/W), which is the highest thermal resistance of insulation materials commonly used in buildings. A higher thermal resistance will enable envelope retrofits in which there is limited space to install the insulation needed to meet building code requirements and in instances in which real estate space is highly valuable. Insulation with a higher thermal resistance are also advantageous to panelized construction because transportation is a significant component of the total cost. Exterior continuous insulation materials that have a higher R-value/in will allow for wall and roof panels that have a thinner profile; thus, more panels can be shipped per truck. Moreover, the dimensions of modular buildings are controlled by transportation limitations, which in turn dictate the dimensions of the living area. Insulation materials with a higher thermal resistance will increase the floor space and height in modular buildings and thus provide a product that is more appealing and valuable to customers.

Author A is a professor in the Department of Mechanical Engineering, Accredited State University, City, State. **Author B** is a research fellow at Commercial Company, City, State.

There are insulation materials with values higher than R6/in (42 m·K/W); however, these have not been adopted by the construction industry for multiple reasons. Aerogels have achieved R8/in (56 m·K/W) and their cost has been decreasing because of new processing methods. Nevertheless, aerogels remain not ideal for buildings because of their fragility. The use of vacuum insulation panels (VIPs) in buildings has been explored by numerous researchers (Alam et al. 2011; Baeten et al. 2010; Nussbaumer et al. 2006; Simmler and Brunner 2005). However, their main hindrance persists: VIPs need to be carefully installed so that the barrier film that maintains the vacuum is not damaged by accidental punctures or cuts. To lessen this concern, Biswas et al. (2018) encapsulated the VIPs in a 4ft×8ft (1.22m×2.44m) polyiso board in which the foam protects the VIPs and provides fastening locations. Also, efforts are underway to develop a self-healing barrier for VIPs that self-repairs in a short time span, so the VIP loses minimal vacuum and maintains its thermal performance (Biswas et al. 2019).

A concept for insulation materials that could outperform aerogels and may be more suitable for construction than VIPs are closed-cell vacuum insulations. It consists of evacuating closed-cells so that if a puncture occurs the damage will be localized and the effect on the effective R-value of the closed-cells is minimal (Fig. 1). The closed-cells can be pores or hollow spheres. Coxe (1971), Henderson (1996), Martin and Pidorenko (1998), and Snowman (1982) developed methods to evacuate microspheres; however, to the best of our knowledge, none of these have been commercialized likely because they are not cost-effective.

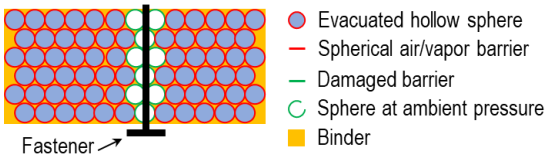

Figure 1 Schematic diagram of evacuated closed cells or spheres assembled with a binder. Damages, such as punctures from a fastener, will cause localized defects that will minimally affect the effective thermal performance. Sketch is not drawn to scale.

The present paper describes ongoing research on two methods to manufacture evacuated spheres: polymeric vacuum insulation spheres (PVISs) and coated and evacuated insulation spheres (CEISs). Both techniques aim to achieve cost-effectiveness by using readily available materials that are easy to process through scalable methods.

METHODOLOGY

Research on PVISs was initiated in October 2017, while work on CEISs started a year later. Thus, more progress and results are available on the former than the latter.

Polymeric Vacuum Insulation Spheres

Figure 2 shows that the proposed manufacturing procedure for PVISs consists of extruding a polymer that is blended with additives. Some of the additives are intended to reduce the thermal conductivity and gas permeability of the polymer. Other additives are desiccant particles that are saturated with water and have the dual purpose of generating pores in the extruded polymer and creating vacuum in the pores. More specifically, during the extrusion process, the polymer encapsulates the desiccant particles and the pressure created by the extrusion process maintains the water inside the desiccant even after the polymer has melted. When the polymer and desiccant exit the extrusion nozzle, pressure on the desiccant particles drops nearly instantaneously, and the water inside the desiccant flashes out as steam and creates pores within the polymer. Afterwards, the water is adsorbed by the desiccant, which creates a vacuum in the pores. Kaufman et al. (2004) followed a similar method to generate vacuum levels <0.001 mbar. Two approaches to produce spheres are being investigated. The first one relies on hot air blowing at the end of an extrusion needle to pull the extruded part at a speed that is faster than the extrusion rate, which separates the extruded part into spheres before the polymer solidifies. The second approach feeds the extruded part with evacuated pores through a mechanical chopper to produce spheres before the polymer solidifies.

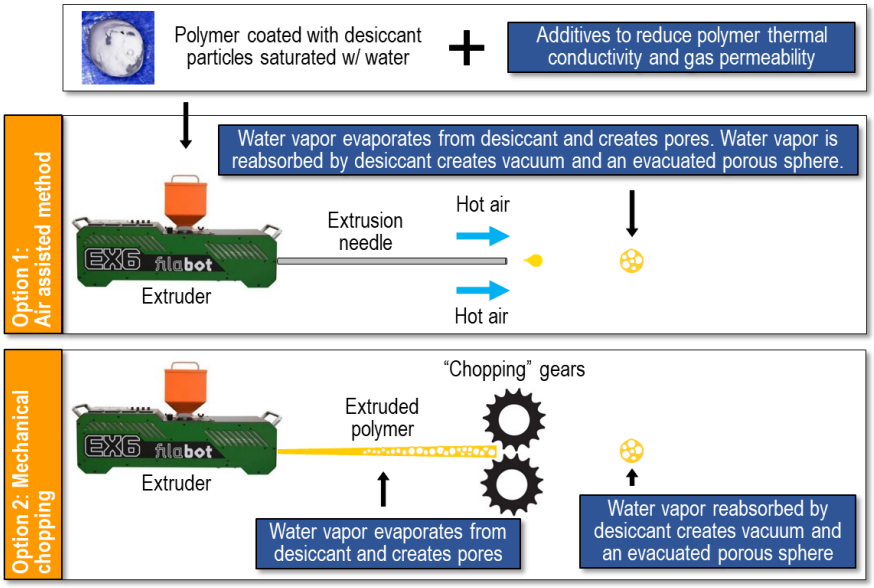

Figure 2 Schematic description of the two approaches being investigated to produce evacuated spheres. Both use desiccant particles that are saturated with water to create pores within the extruded polymer and evacuate the pores. They differ in how the spheres are produced from the extruded part. The first option uses hot air to pull the extruded part into spheres. The second option uses gears to cut the extruded part into spheres.

Table 1 lists the approximate values of the key parameters needed to achieve spheres that could have ~R22/in (153 m·K/W) and an effective thermal performance of ~R14/in (97 m·K/W) after the evacuated spheres are assembled into a board using polyiso foam as the binder. The targets were estimated based on equations from Russell (1935); these were selected among a multitude of options in the literature (Shrestha et al. 2019) because their relative simplicity allowed for quick estimations.

Table 1. Targeted parameters for the polymeric vacuum insulation spheres to achieve an effective thermal performance of ~R14/in (97.1 m·K/W).

Parameter	Targets	Status
Sphere diameter (inches, μm)	7.9E-3 (200)	≤ 1.4E-2 (350)
Void fraction within sphere (%)	≥ 90	≥ 70
Void fraction within binder (%)	≥ 70	-
Pore diameter (inches, μm)	4E-4 – 8E-4 (10 – 20)	≤ 2E-3 (50)
Pressure inside pore (atm, mbar)	9.9E-3 – 9.9E-4 (0.1 – 1)	9.9E-2 ≤ (100)
Polymer thermal conductivity (Btu/h·ft·°F, W/m·K)	≤ 0.058 (0.1)	0.069 (0.12)
Polymer OTR (in^3/ft^2·day, $cm3/m^2$·day)	~2.83E-5 (0.005)	2.27E-4 (0.04)
Shell thickness (inches, μm)	4E-5 – 8E-5 (1 – 2)	2E-4 ≤ (5)
R-value/in without binder ($h·ft^2·°F$/Btu·in, m·K/W)	≥ 22 (153)	≥ 5 (35)
R-value/in with binder[a] ($h·ft^2·°F$/Btu·in, m·K/W)	≥ 14 (97)	-

a. Thermal properties of polyiso foam (i.e., R6/in (41.6 m·K/W) were used for the binder.

Two main tasks are being performed to assess the proposed manufacturing procedure:

Task 1: Polymer tailoring

1. Selection of polymers: Relatively low thermal conductivity, relatively low cost, low or no toxicity, and modulus of elasticity ≥2.2E5 psi (1.5 GPa) so the thin walls of the pores do not collapse under negative pressure. Also, the polymer needs to flow at the processing temperature, which means that the glass transition temperature (T_g) and the melting temperature (T_m) of the polymer must be lower than the typical processing temperature of ~212°F (100°C).
2. Selection of desiccants: Low cost, low or no toxicity, and immiscibility with the selected polymer(s).
3. Evaluation of extrusion temperatures, extrusion rates, and nozzle sizes.
4. Selection and evaluation of additives that decrease thermal conductivity and gas permeability of

polymer(s): Low thermal conductivity, low cost, low or no toxicity, and miscibility with polymer(s).

Task 2: Sphere production

The following subtasks are being executed:

1. Assessment of the air assisted method
2. Evaluation of the mechanical chopping method

Bench-scale extrusion trials are being performed with either a Filabot EX2 or EX6. Preliminary evaluations of pore morphology in the extruded parts (e.g., uniformity, size, wall thickness, etc.) are being conducted by examining scanning electron microscopy (SEM) images.

Coated and Evacuated Insulation Spheres

The proposed manufacturing process for CEISs uses naturally-occurring or synthesized hollow micro particles or spheres. The spheres should have porous walls for gas to more easily diffuse through the shell and enable evacuation of the spheres. To maintain vacuum, coating agents are being investigated to fill the pores of the shell via wicking of the coating into the pores due to capillary forces or conformably coat the shell surface. The thickness of the coating will be as thin as possible to reduce thermal conductivity and maintain vacuum within the spheres.

Polymeric or organic coatings are being evaluated because they have relatively low thermal conductivity, are economical, can be dissolved in eco-friendly solvents, and can be applied via simple and scalable methods such as dip coating. Three dip coating procedures are being evaluated:

1. Dip coating with heating: add 0.17 fl oz (5 ml) polymer solution and 0.0017 oz (50 mg) of microspheres to 0.68 fl oz (20 ml) vail, heat at 176°F (80°C) for 24 h to accelerate molecular movement and enhance mixing, centrifuge at 7000 rpm for 10 minutes to remove excess solution, add more solvent and wash twice to remove "free polymer, and dry overnight at room temperature.
2. Dip coating with 200 rpm shaking: add 0.17 fl oz (5 ml) polymer solution and 0.002 oz (60 mg) of microspheres to 0.68 fl oz (20 ml) glass vial, shake at 200 rpm for 24 h, centrifuge at 7000 rpm for 10 minutes, wash three times with solvent to remove excess polymer, and dry overnight at room temperature.
3. Dip coating with 800 rpm shaking: add 0.17 fl oz (5 ml) solution and 0.002 oz (60 mg) of microspheres to 1.7 fl oz (50 ml) tubes, shake at 800 rpm for 24 h, centrifuge at 7000 rpm for 10 minutes, wash three times with solvent, and dry overnight at room temperature.

After air drying overnight, the spheres are placed in a vacuum oven at 356°F (180°C) for three hours to evacuate the spheres and to anneal the coating through thermal treatment.

The main tasks that are being performed to assess the proposed manufacturing procedure are:

1. Selection of hollow microspheres with porous shells.
2. Selection of coating candidates: Relatively low thermal conductivity, high potential for physical and/or chemical bonding with the spheres, and soluble in environmentally friendly and commercially viable solvents.
3. Evaluation of dip coating method and densification of coating in vacuum oven by SEM and energy dispersive X-ray (EDAX) analysis.

RESULTS AND DISCUSSION

Polymeric Vacuum Insulation Spheres

Selection of polymer. We conducted preliminary trials with acrylonitrile butadiene styrene (ABS), high-density polyethylene (HDPE), polypropylene (PP), polystyrene (PS), and polymethyl methacrylate (PMMA). Although these polymers appeared promising, we selected to continue our evaluations with PMMA because of its relatively high

Young's modulus ~4.8E5 psi (~3.3 GPa) and relatively low thermal conductivity (~0.11 Btu/h·ft·°F, 0.195 W/m·K).

Selection of desiccant (i.e., blowing agent and vacuum generator). We selected zeolite particles, and in particular 3A and Y74, as the desiccant because these are economical and readily available. The zeolites that we are currently using have diameters of about 2E-4 inches (5 μm); future experiments will involve smaller particles given that we are targeting pores in the 4E-4 to 8E-4 inches (10 to 20 μm) range. We saturated the zeolite with water by loading the zeolite with water at 50% wt. ratio, which exceeds the water uptake limit of the zeolite, and waiting for ~30 minutes for the water to be adsorbed by the desiccant. The zeolite was then heated to 131°F (55°C) to remove excess water, which does not affect the water that had been adsorbed by the porous structure of the zeolite because it needs to be heated to ~302°F to 392°F (150°C to 200°C) for it to desorb. This in turn means that the extrusion temperature must be ≥ 392°F (200°C) so that water vapor desorbs from the zeolite and creates pores in the polymer.

For more uniform mixing of the desiccant and the polymer, we mixed them before we added them to the extruder. To this end, we added the polymer pellets to a rotary tumbler, sprayed them with a 1% aqueous solution of polyvinylpyrrolidone (PVP), and slowly added the zeolite particles to coat the pellets while these were still tumbling.

Initial extrusion trials with selected polymer and desiccant. We used a Filabot EX2 extruder with various nozzle sizes to investigate extrusion parameters such as polymer/zeolite ratio, type of zeolite, and extrusion temperature and speed. Prior to extrusion, the PMMA and zeolite were heated overnight at 140°F (60°C) under vacuum to remove all the water and gas contained in the raw materials. Before extrusion, the zeolite particles were saturated with water and the excess water was removed by heating the desiccant at 131°F (55°C) for 30 minutes.

We studied the effect of temperature by extruding PMMA/zeolite Y74 at 10:1 weight ratio at an extrusion speed of ~17 rpm or 50% of the Filabot EX2 maximum extrusion speed. Extrusion with a 2.36E-2 -inch (600 μm) diameter nozzle at 419°F (215°C) lead to a part that was ~3.94E-2 inches (1 mm) in diameter; that is, it expanded in size by a factor of ~1.7. High expansion is a potential indicator of vacuum level inside the pores because the amount of expansion is proportional to the amount of water that evaporated from the zeolite, and a higher vacuum is likely to be produced because more water is adsorbed back into the zeolite. Additional trials suggest that parts had more uniform pore sizes and expanded by a factor of ~1.5 when the extrusion temperature was 428°F (220°C). Future experiments will seek to balance vacuum level and pore size uniformity.

Experiments were also conducted to confirm that the water capacity of different zeolite types affects the size of the pores that they produce. Separate trials were performed in which PMMA was combined with zeolite 3A and Y74 at a 10:1 weight ratio. Parts were extruded with a 2.36E-2 -inch (600 μm) nozzle at 428°F (220°C) and 50% extrusion speed. Figure 3 illustrates that because zeolite 3A has a higher water capacity, pores were ~5.12E-3 inch (130 μm) in diameter. In contrast, pore diameters were ~1.97E-3 inch (50 μm) or about 60% smaller with zeolite Y74. To achieve the targeted 3.94E-4 to 7.87E-4 -inch (10 to 20 μm) pores, we will have to either tailor the water loading in the zeolite particles or use zeolite particles that are smaller than the current 1.97E-4 inch (5 μm) so that less water is released by the desiccant. Future work will involve determining the amount of water needed to create the < 7.87E-4 -inch (20 μm) pores and adequate vacuum.

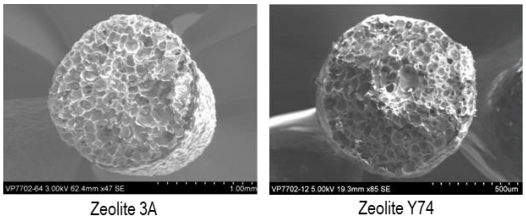

Figure 3 Filaments extruded with a 2.36E-2 -inch (600 μm) nozzle using PMMA, and zeolite 3A (left) or zeolite Y74 (right) at 10:1 weight ratio and 428°F (220°C) extrusion temperature.

Additives that decrease the thermal conductivity and gas permeability of polymers. We examined the effect of inorganic materials on the gas permeability and conductivity of polymers based on research by Priolo et al (2010), Guin et al. (2014), and Kim et al (2012). We selected CLOISITE-Na+, also known as nanoclays, because it is

readily available and economical, and because it is miscible with PMMA.

To perform preliminary studies on the effect of nanoclays on the gas permeability of PMMA, we prepared three 7.9× 7.9×0.016-inch (20 cm × 20 cm × 400 μm) samples by solvent casting from chloroform: (1) raw PMMA, (2) PMMA with 10 wt% CLOISITE-Na+, and (3) PMMA with 20 wt% of CLOISITE-Na+. We did not use an optimized mechanism to create the gas barrier (i.e., careful layout of nanoclay layers) because we wanted to conduct a cursory evaluation. Mocon Inc. measured the oxygen transmission rate (OTR) of the samples according to the test standard ASTM F1927 at 77°F (25°C), at 50% relative humidity and 1 atm (1013 mbar). Table 2 shows that 10% and 20% by wt. of CLOISITE-Na+ decreased the OTR of PMMA from 1.6 $in^3/ft^2 \cdot day$ (282 $cm^3/m^2 \cdot day$) to 1.0 $in^3/ft^2 \cdot day$ (181 $cm^3/m^2 \cdot day$) and 0.8 $in^3/ft^2 \cdot day$ (140 $cm^3/m^2 \cdot day$), respectively. Although a decrease of 52% was encouraging, the OTRs are far from the targeted 2.83E-5 $in^3/ft^2 \cdot day$ (0.005 $cm^3/m^2 \cdot day$) needed to maintain the vacuum inside the spheres as indicated in Table 1. We have several options to decrease the OTR; these include using ethylene vinyl alcohol (EVOH), which has a gas permeability that is ~3 orders of magnitude lower than PMMA.

Table 2. Effect of CLOISITE-Na+ on the oxygen transmission rate of PMMA.[a]

Sample	Oxygen transmission rate ($in^3/ft^2 \cdot day$, $cm^3/m^2 \cdot day$)	% Decrease
PMMA	1.6 (282)	-
PMMA 10 wt% Cloisite-Na+	1.0 (181)	42
PMMA 20 wt% Cloisite-Na+	0.8 (140)	52

a. Measurements collected according to ASTM F1927 at 77°F (25°C), 50% relative humidity, and 1 atm (1013 mbar).

We also prepared 4.5×4.5×0.35-inch (11.4×11.4×0.9 cm) samples to examine the effect of nanoclays on thermal conductivity. The samples were prepared by melt pressing polymer pellets with and without Cloisite-Na+ at 311°F (155°C) under the pressure of 1000 psi (6.9 MPa). One sample was made of raw PMMA and the other was PMMA with 20 wt% Cloisite-Na+. The measured thermal conductivities were 0.08 Btu/h·ft·°F (0.14 W/m·K) and 0.069 Btu/h·ft·°F (0.12 W/m·K), respectively, which puts us close to our target of 0.058 Btu/h·ft·°F (0.1 W/m·K). Further evaluations will include lowering the thermal conductivity by increasing the nanoclay loading.

Sphere production via the air assisted method. We conducted experiments using a Filabot EX6 extruder and PMMA with 5 wt% zeolite 3A. The effectiveness of this method is highly dependent on flow rate and temperature of the air that is pulling the extruded part from the nozzle. Incorrect settings yielded the elongated pieces shown in Figure 4. After numerous trials we produced ~3.94E-3 -inch (100 μm) spheres shown in Figure 4. However, we were not able to consistently repeat the process with our limited bench-scale setup. Nevertheless, these results should suffice as a successful proof of concept that an industry could perfect to mass produce PVISs.

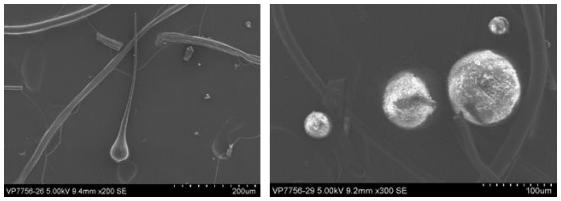

Figure 4 Extruded parts manufactured using the air assisted method and PMMA with 5 wt% zeolite 3A. Left: elongated parts produced when the flow rate and temperature of the air were not correct. Right: sphere prototypes.

Sphere production via the chopping method. We performed initial trials with a single "chopping" gear to expedite the decision about the viability of the proposed procedure. Two "chopping" gears would have required more preparation time because these would likely have to be specially ordered so that the teeth precisely match each other. Figure 5 shows that the zeolite produced a porous part; however, the single gear did not produce individual spheres. Nonetheless, the preliminary trials suggest that with the appropriate teeth and setup design that we may be able to produce spheres with a single gear, which will greatly simplify the manufacturing system. Thus, our ongoing efforts are focusing on evaluating the single gear approach.

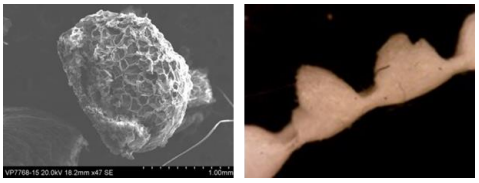

Figure 5 Extruded parts manufactured using the "chopping" method with a single gear and PMMA with 5 wt% zeolite 3A. The left image shows high porosity in the extruded part, although the right image shows that the preliminary single gear setup did not yield separate spheres.

Table 1 summarizes where the research stands with respect to the parameters being targeted to achieve the desired thermal resistance. Gas permeability and pressure inside the pores will be the most challenging ones to attain.

Coated and Evacuated Insulation Spheres

Selection of hollow particles. We decided to start our experiments with hollow glass microspheres that have porous walls from Mo-Sci Corporation because the shells have a nanostructure of interconnected pores. This type of structure is crucial to be able to evacuate the spheres when placed in a vacuum chamber. Figure 6 shows that the spheres range in diameter from 1.57E-3 to 3.54E-3 inches (40-90 μm), have a ~3.94E-5 -inch (1 μm) thick shell, and the pores in the shell range from 3.94E-7 to 1.18E-5 inches (10 to 300 nm).

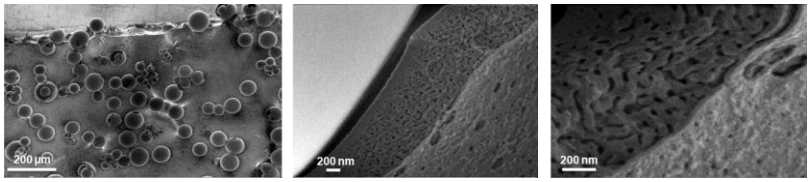

Figure 6 SEM images of the hollow glass microspheres and the typical cross-sectional nanostructure of the interconnected porous shell.

Selection of organic coating and evaluation of dip coating methods. Our polymer selection was based on commercial availability and solubility in environmentally benign solvents. We used these polymers in solutions that had a concentration of 6.68 oz/gal (0.05 g/mL) to perform preliminary assessments of the uniformity of the coatings that the three dip coating methods produced. These qualitative evaluations were conducted by examining SEM and EDAX images. As described in Table 3, the methods in which the polymer solution and the particles were either heated or shaken at 200 rpm did not provide consistent results. However, relatively uniform coatings were obtained with Elvacite 2018, Mowitac B60H, and PVB 98 when the polymer solution and the particles were shaken at 800 rpm. Thus, we chose to continue the evaluations with these three polymers and the 800-rpm mixing method, and decided to add polyvinyl alcohol (PVA) because of its relatively low gas permeability and it is soluble in water.

Table 3. Results from dip coating methods.

Coating material[a]	Solvent	Dip coating method	Findings
Acryloid B-72 (ethyl methacrylate co-polymer)	Ethanol	Heating	Uniform coating
Elvacite 2028 (low molecular weight methacrylate copolymer)	Ethanol	Heating	Uniform coating
	Ethanol	200 rpm shaking	Difficult to control and reproduce
	Ethanol	800 rpm shaking	Relatively uniform coating
Mowital B60H (polyvinyl butyral)	Ethanol	800 rpm shaking	Relatively uniform coating
Poly (MMA-*co*-EA)	Tetrahydro-furan	Heating	Nonuniform coating
	Tetrahydro-furan	200 rpm shaking	Difficult to control and reproduce
Polystyrene (PS)	Tetrahydro-furan	Heating	Non-uniform surface coverage
	Tetrahydro-furan	200 rpm shaking	Difficult to control and re-produce
PVB 98 (polyvinyl butyral)	Ethanol:toluene (40:60)	800 rpm shaking	Relatively uniform coating
QPAC 25 (poly (ethylene carbonate))	Ethanol	800 rpm shaking	Nonuniform coating. Different solvent may be needed.

a. Polymer solutions had a concentration of 6.68 oz/gal (0.05 g/mL).

Table 4 provides more details about the four selected polymers. They have thermal conductivities that are ≤

0.116 Btu/h·ft·°F (0.2 W/m·K). Moreover, PVB 98 and Mowital B60H are commercially utilized as binders, which could facilitate adhesion to the shell of the spheres, and Elvacite 2028 is highly durable and chemically resistant. Table 4 also shows that the glass and melting point temperatures for these polymers ranged from 140 to 365°F (60 to 185°C); thus, the annealing temperature needs to stay within this range.

Table 4. Selected organic coating materials.

Polymer	Thermal conductivity (Btu/h·ft·°F, W/m·K)	T_g (°C)[a]	T_m (°C)[a]	Common Applications
PVB 98	0.116 (0.2)	63	N/A	Binders
Elvacite 2028	0.058 - 0.116 (0.1 - 0.2)	62	130	Ink, lacquers and metal coatings
Mowital B60H	0.116 (0.2)	61	136	Binder for coatings, printing inks, ceramics
PVA	0.116 (0.2)	85	185	Textiles, coatings

a. Glass transition temperature (T_g) and melting point (T_m) were determined by differential scanning calorimetry.

Preliminary results. We conducted annealing trials of glass microspheres that were coated with polymer solutions with a concentration of 6.68 oz/gal (0.05 g/mL). Annealing was performed at 356°F (180°C) for three hours. Figure 7 shows how the uniformity of the Elvacite 2028 coating improved after annealing.

We increased the concentration of the polymer solution to 13.4 oz/gal (0.1 g/mL) to check the effect of concentration on coating quality. To evaluate the quality of the coatings, we conducted EDAX analysis of their surfaces that show the color-coded elemental maps for each polymer system. The coated particles revealed a strong carbon (C) signal due to the polymeric layer that was comparable to the silica (Si) signal that is associated with the glass microspheres, which suggests dense polymer coverage over the shell of the spheres. Figure 8 shows images after the polymeric coatings were annealed at 356°F (180°C) for three hours in a vacuum furnace at ~7.9E-5 atm (8E-2 mbar). PVB 98 and PVA appear to be denser and more uniform; which is corroborated by the strong carbon signal shown in the EDAX images. However, the spheres coated with Elvacite 2028 and Mowital B60H showed a somewhat weaker carbon signal after thermal treatment, suggesting that the annealing conditions need optimization.

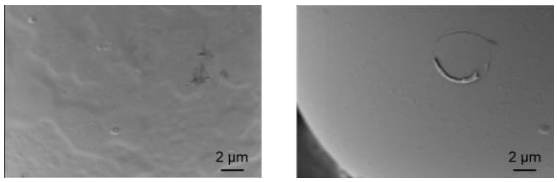

Figure 7 SEM of a glass microsphere coated with Elvacite 2028 before (left) and after (right) annealing at 356°F (180°C) for three hours.

NEXT STEPS

Upcoming tasks relevant to PVIS and CEIS include developing a bench-scale setup to measure the pressure inside the spheres. A tentative scheme involves connecting a pressure gauge to an airtight vessel, adding a considerable amount of evacuated spheres to the vessel, and observing changes in pressure with time. Measurements will provide guidance on the effectiveness of the evacuation methods and the gas permeability of materials supposed to maintain vacuum within the spheres. Other tasks include developing ways to effectively integrate the evacuated spheres into building envelopes.

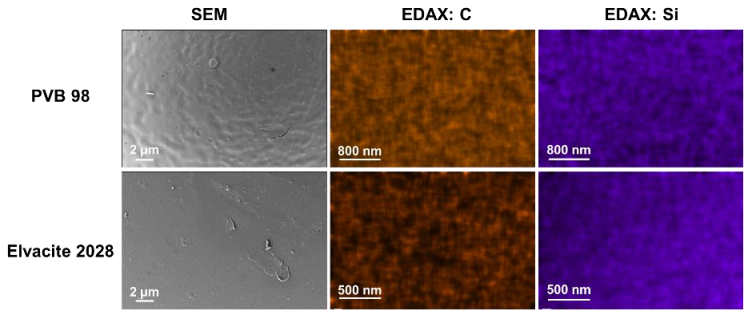

Figure 8 SEM and color-coded EDAX elemental maps of polymer coated microspheres after annealing through thermal treatment. Dark orange indicates the presence of carbon (i.e., polymer) and purple silica (i.e., glass).

Polymeric Vacuum Insulation Spheres

Some of the upcoming tasks to continue developing and evaluating the method to manufacture the PVIS are:

1. Demonstrate that the "chopping" method with a single gear can produce single spheres and that the method can be modified to control the sphere diameter.
2. Determine the polymer to zeolite ratio and the water content level in the zeolite needed to achieve pores that are < 7.87E-4 inches (20 μm) in diameter and have the required vacuum level.
3. Evaluate the processability of ethylene vinyl alcohol (EVOH) with zeolites and nanoclays because it has a lower gas permeability than PMMA.
4. Measure the porosity of the spheres according to ASTM D6226.
5. Continue making progress toward the targets listed in Table 1 and modify these targets as the process to manufacture PVIS and achieve the desired thermal resistance is optimized.

Coated and Evacuated Insulation Spheres

Some of the tasks to continue developing and evaluating the proposed method are:

1. Continue evaluating the dip coating and annealing procedures with organic coating materials.
2. Determine the required thickness for the organic coating and porous glass shell to retain vacuum.
3. Assess the possibility of coating the microspheres with inorganic materials because these have a much lower gas permeability than organic materials. Disadvantages of inorganic coatings include higher cost; thermal expansion mismatch between the inorganic coating and the shell could lead to crack formation; and potentially more expensive processes to coat the particles such as sputtering deposition.

CONCLUSION

Progress has been made toward developing cost-effective manufacturing procedures for evacuated spheres. The method to manufacture polymeric vacuum insulation spheres shows advantages from the perspective of mass production and the use of economical materials and equipment that are readily available. Upcoming challenging tasks include identifying economical mechanisms to maintain the vacuum within the spheres and finding the optimized settings to generate the desired pore sizes with the needed vacuum level. Benefits from the method to produce coated and evacuated insulation spheres include the use of readily available materials and processing methods that are scalable. Future challenging tasks include tailoring the thickness of the coating to both reduce thermal conductivity and maintain vacuum within the spheres. Potential paths to address these challenges are currently ongoing.

ACKNOWLEDGMENTS

The authors would like to thank the U.S. Department of Energy for funding this research. This manuscript has been authored by UT-Battelle, LLC, under Contract No. DE-AC05-00OR22725 with the U.S. Department of Energy.

REFERENCES

Alam, M., Singh, H., and M.C. Limbachiya. 2011. Vacuum Insulation Panels (VIPs) for building construction industry – A review of the contemporary developments and future directions. *Applied Energy* 88(11):3592-3602.

Baetens, R., Jelle, B.P., Thue, J.V., Tenpierik M.J., Grynning, S., Uvsolkk, S., and A. Gustavsen. 2010. Vacuum insulation panels for building applications: A review and beyond. *Energy and Buildings* 42(2):147-172.

Biswas, K., Desjarlais, A., Smith, D., Letts, J., Yao, J., and T. Jiang. 2018. Development and thermal performance verification of composite insulation boards containing foam-encapsulated vacuum insulation panels. *Applied Energy* 228(15):1159-1172.

Biswas, K., Gilmer, D., Ghezawi, N., Cao, P., and T. Saito. 2019. Demonstration of self-healing barrier films for vacuum insulation panels. *Vacuum* 164:132-139.

Coxe, E.F. 1971. Method for producing evacuated glass microspheres. US Patent 3,607,169.

Guin, T., Krecker, M., Hagen, D.A., and J.C. Grunlan. 2014. Thick growing multilayer nanobrick wall thin films: super gas barrier with very few layers. *Langmuir* 30:7057-60.

Henderson, T.M. 1996. Thermal Insulating Material and Method of Manufacturing. US Patent 5,500,287.

Kaufman, J.W., Klett J.W., Klett L., and J. Armstrong. 2004. Advanced man-mounted heat-pipe for portable cooling. *In: Proceedings of the 34th International Conference on Environmental Systems.*

Kim, E., Jeong S.Y., Shin, G., Lee, S., and K.H. Choi. 2012. Properties of thermal conductivity on polyimide/clay nanocomposite foams. *Applied Mechanics and Materials* 229-331:215-218.

Martin, A.J., and J. Pidorenko. 1998. Insulation microspheres and method of manufacture. US Patent 5,713,974.

Nussbaumer, T., Ghazi Wakili, K., and C. Tanner. 2006. Experimental and numerical investigation of the thermal performance of a protected vacuum-insulation system applied to a concrete wall. *Applied Energy* 83(8):841-855.

Priolo, M.A., Gamboa, D., Holder, K.M., and J.C. Grunlan. 2010. Super gas barrier of transparent polymer − Clay multilayer ultrathin films. *Nano Letters* 10:4970–4974.

Russell, H.W. 1935. Principles of heat flow in porous insulators. *J American Ceramic Society* 18:1-5.

Shrestha, S.S., Rai, A., Feng, T., Zhang, M., Hun, D., Biswas, K., and A. Desjarlais. 2019. Review of models to evaluate and guide the development of low thermal-conductivity materials. *In: Proceedings of the 2019 Buildings XIV International Conference. Clearwater, FL.*

Simmler, H., Brunner, S. 2005. Vacuum insulation panels for building application: Basic properties, aging mechanisms and service life. *Energy and Buildings* 37(11):1122-1131.

Sowman H.G. 1982. Non-vitreous ceramic metal oxide microcapsules and process for making same. US Patent 4,349,456.

Willems, W.M., and Schild, K. 2005. Vacuum insulated constructions in detail, in: *Proceedings of the 7th Symposium on Building Physics in the Nordic Countries, IBRI, Reykjavik, 928–936*.